Structural Transformation, Intermediate-Range Order, and Dynamical Behavior of SiO_2 Glass at High Pressures

Wei Jin, Rajiv K. Kalia, and Priya Vashishta

Concurrent Computing Laboratory for Materials Simulations, Department of Physics and Astronomy and Department of Computer Science, Louisiana State University, Baton Rouge, Louisiana 70803-4001

José P. Rino

Universidade Federal de São Carlos, 13560 São Carlos, São Paulo, Brazil

(Received 23 November 1992)

Pressure-induced structural transformation in SiO_2 glass is investigated with molecular dynamics. At high densities, the height of the first sharp diffraction peak is considerably diminished, its position changes from 1.6 to 2.2 $Å^{-1}$, and a new peak appears at 2.85 $Å^{-1}$. At twice the normal density, the Si-O bond length increases, the Si-O coordination changes from 4 to 6, and the O-Si-O band angle changes from 109° to 90°. This is a tetrahedral to octahedral transformation, which was reported recently by Meade, Hemley, and Mao [Phys. Rev. Lett. **69**, 1387 (1992)]. Results for phonon density of states also reveal significant changes at high pressures.

PACS numbers: 61.43.Bn, 61.43.Fs, 62.50.+p, 63.50.+x

Over the years, SiO_2 has been the focus of many investigations in solid state physics, microelectronics, geosciences, materials science, and engineering [1–12]. In the past decade, numerous attempts have been made to investigate the structure and dynamics of crystalline and glassy states of SiO_2 at high pressures [11–24]. Brillouin [11], Raman [11–13], infrared [12,14], neutron [15], and x-ray [16] scattering techniques have been used to investigate pressure-induced effects in SiO_2 glass. At high pressures, irreversible changes, indicating permanent densification, have been observed in the Brillouin and Raman spectra [11] of recovered SiO_2 glass samples. Infrared absorption measurements [14], however, indicate reversible changes in the SiO_2 glass at 20 GPa.

Recently Meade, Hemley, and Mao [16] have carried out *in situ* high-pressure (8–42 GPa) x-ray diffraction experiments on SiO_2 glass. These measurements reveal significant changes in the short-range and intermediate-range order (IRO). The position of the first sharp diffraction peak (FSDP) in x-ray structure factor, the fingerprint of IRO, changes from 1.55 $Å^{-1}$ at 8 GPa to 2.37 $Å^{-1}$ at 42 GPa. At the same time, there is a significant decrease in the height and an increase in the width of the FSDP. Furthermore, the pair correlation function shows that the nearest-neighbor (nn) tetrahedral coordination of Si-O changes to octahedral coordination as the pressure is increased from 8 to 42 GPa. Raman and infrared spectra at pressures greater than 28 GPa reveal the absence of tetrahedral vibrational modes [13,14].

In this Letter, we describe the molecular-dynamics (MD) simulation results for the effect of high pressure on structural correlations and phonon density of states of SiO_2 glass. These simulations cover a range of pressures over which the mass density of the system changes from 2.20 (normal density) to 4.28 g/cm^3. This twofold increase in the density produces a loss of the intermediate-range order and a structural transformation from corner sharing $Si(O_{1/2})_4$ tetrahedral network at normal density to a corner and edge sharing network of $Si(O_{1/3})_6$ octahedra at the highest density.

Molecular-dynamics simulations were performed with interatomic potentials comprising two- and three-body terms [9]. The two-body potentials combine steric repulsion, long-range Coulomb interaction due to charge-transfer effects, and charge-dipole interaction due to large electronic polarizability of O^{2-} ions. The three-body covalent interactions include the effects of bond bending and stretching [25]. The MD simulations were carried out for 648-particle (216 Si and 432 O) systems at normal mass density $\rho_0 = 2.20$ g/cm^3, and at pressures 0.9, 5.4, 22.7, and 42.3 GPa, corresponding to densities $\rho = 2.64$, 2.94, 3.53, and 4.28 g/cm^3, respectively. Periodic boundary conditions were employed and the long-range nature of the Coulomb interaction was taken into account by Ewalds's summation.

The SiO_2 glasses were generated by quenching well equilibrated liquids at high temperatures (~4000 K) [9]. High-pressure SiO_2 glasses were also prepared in a similar fashion except that the length of the MD cell and atomic positions were first appropriately scaled in high-temperature liquid states. Low-temperature glasses were further relaxed with the aid of the steepest-descent quench [9]. At each temperature and density, structural and dynamical correlations were calculated with MD trajectories of at least 30 ps.

In Fig. 1, we present the MD results for the density dependence of the static structure factor, $S(q)$. In the normal density glass, the FSDP is located at 1.6 $Å^{-1}$. With an increase in the density, the height of the FSDP decreases, its width increases, and its position shifts to higher values of q. Note that simple elastic compression [i.e., $(\rho/\rho_0)^{1/3}$] cannot account for the observed shift in

0031-9007/93/71(19)/3146(4)$06.00

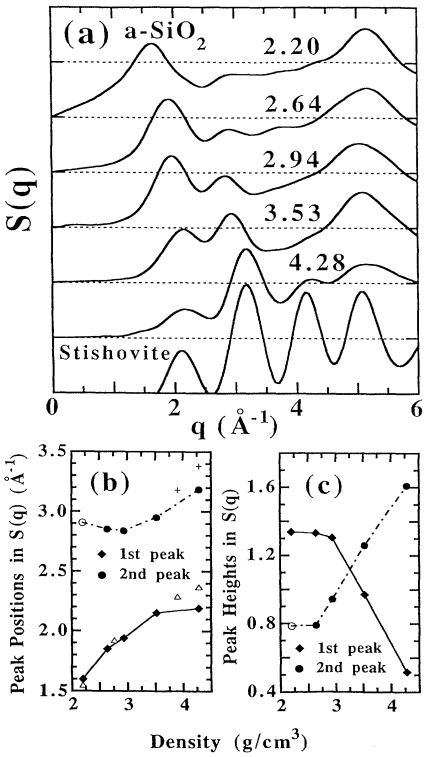

FIG. 1. (a) Molecular-dynamics results for the static structure factor, $S(q)$, of normal and high density SiO_2 glasses at 300 K; (b) density dependencies of positions of the first two peaks in $S(q)$; (c) density dependencies of heights of the first two peaks in $S(q)$. In (b) and (c), open circles at normal density are meant to indicate that the second peak is broad and has a small amplitude. Triangles and crosses in (b) represent the experimental data estimated from Ref. [16].

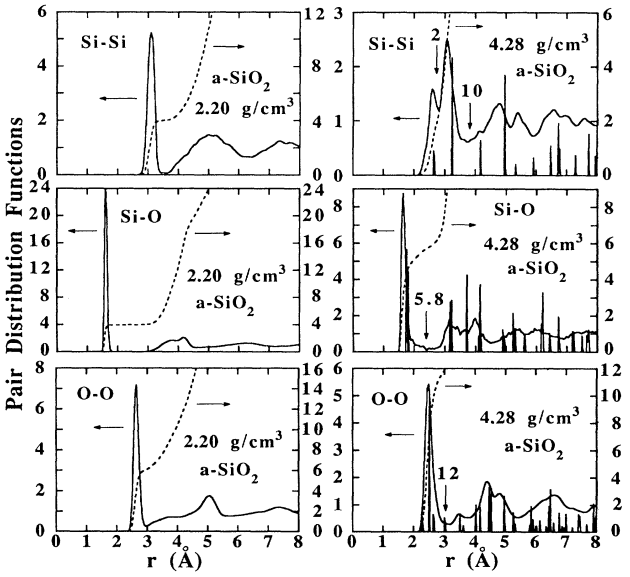

FIG. 2. MD partial pair-distribution functions (solid lines) and coordination numbers (dotted lines) for SiO_2 glasses at normal and stishovite densities at 300 K. Sharp peaks at 4.28 g/cm^3 correspond to pair-distribution functions for crystalline stishovite.

the position of the FSDP. Elastic compression corresponding to density increases of 20%, 33%, 60%, and 95% would shift the FSDP to 1.71, 1.77, 1.88, and 2.01 Å^{-1} whereas the simulation results reveal higher values for the position of the FSDP: 1.85, 1.94, 2.15, and 2.19 Å^{-1}. The high-pressure x-ray measurements by Meade, Hemley, and Mao [16] reveal similar behavior for the FSDP.

Figure 1 also shows a new peak in the static structure factor. It appears when the density of the normal system is increased by 20%. Located at 2.85 Å^{-1}, the peak grows with further increase in the density. However, its position shifts only slightly at higher pressures [Fig. 1(b)]. These results are again well supported by the recent x-ray measurements at high pressures [16].

Partial pair-distribution functions $g_{\alpha\beta}(r)$ at the normal and the highest densities are shown in Fig. 2. The position of the first peak in $g_{Si\text{-}O}(r)$ and the corresponding Si-O coordination remain unchanged up to 3.53 g/cm^3. At a pressure of 42.3 GPa where the glass density (4.28 g/cm^3) reaches the stishovite density, the first peak in $g_{Si\text{-}O}(r)$ occurs at 1.67 Å instead of 1.61 Å and the Si-O coordination increases from 4 to 5.8. In stishovite, the highest density crystalline phase of SiO_2, Si-O bond lengths are 1.76 and 1.81 Å and the Si-O coordination is 6. In the glass at 4.28 g/cm^3, the second peak in $g_{Si\text{-}O}(r)$ is at 3.15 Å, close to the next-nearest-neighbor (nnn) Si-O distance ($\sim$3.20 Å) in the stishovite.

Figure 2 also shows how the Si-Si pair-distribution function changes upon densification. The first peak splits into two peaks when the density increases to 4.28 g/cm^3. One of these peaks is located at 2.59 Å, close to the nearest-neighbor Si-Si distance (2.67 Å) in the stishovite. The second peak appears at 3.07 Å which is close to the nnn Si-Si distance (3.24 Å) in the stishovite. The area under the first peak gives a coordination of 2 while the area under the first two peaks is 10. At normal density, the nn O-O coordination is 6. It increases to 10 at 3.53 g/cm^3 and to 12 at 4.28 g/cm^3. In stishovite crystal, the O-O coordination is 12.

Figure 3 displays the MD results for O-Si-O and Si-O-Si bond-angle distributions in SiO_2 glasses at different densities. As the density increases, the peaks in these distributions broaden and also shift to lower angles because of increased distortions of $Si(O_{1/2})_4$ tetrahedra. At normal density, the O-Si-O distribution has a peak at 109° with a full width at half maximum (FWHM) of 10°. With a 20% increase in the density, this peak moves to 107° and the FWHM increases to 12°. Further increase of 40% in the density shifts the peak to 104° and increases the FWHM to 17°. However, there is a dramatic

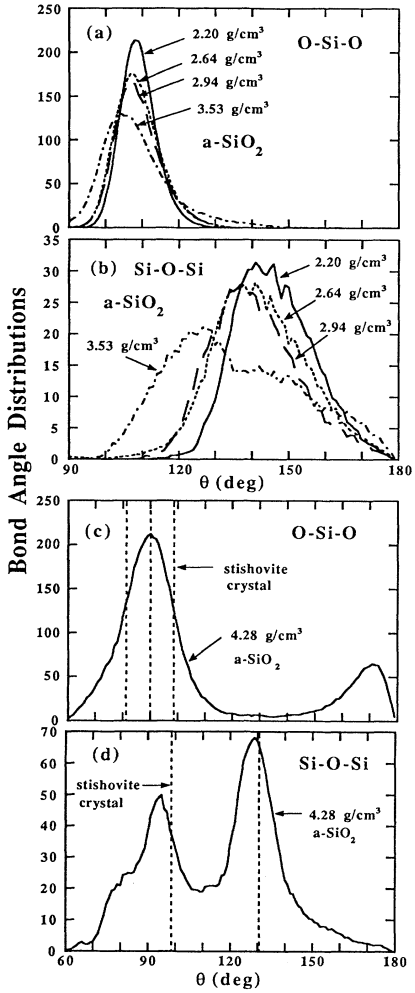

FIG. 3. O-Si-O and Si-O-Si bond-angle distributions for normal and high density SiO_2 glasses.

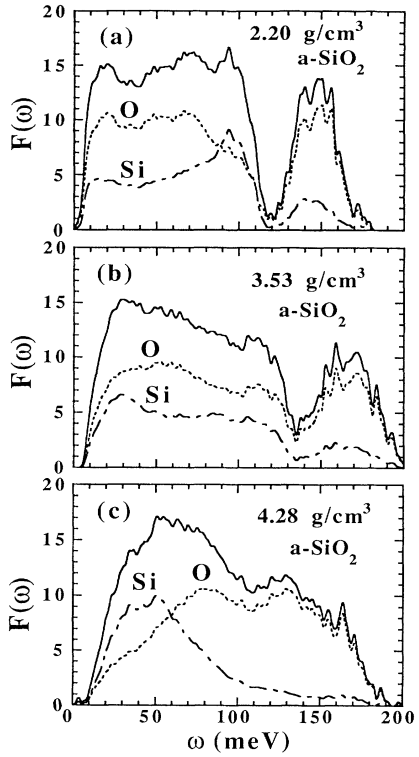

FIG. 4. Partial and total phonon density of states for normal and high density SiO_2 glasses.

change in the distribution when the glass density reaches the stishovite density: The O-Si-O distribution has a broad peak at 90°. In the crystalline stishovite, on the other hand, the O-Si-O angles are 81.35°, 90°, 98.65°, and 180°.

In the normal density SiO_2 glass, the Si-O-Si bond-angle distribution has a peak at 142° and the FWHM of this peak is 26° (Fig. 3). Both of these results are in excellent agreement with NMR measurements [7]. With a density increase of 33%, this peak shifts gradually to 137°. With 60% densification, the peak moves to 127° and a broad shoulder appears between 135° and 150°. At the stishovite density, the Si-O-Si bond angle in the glass has broad peaks around 95° and 128°. These values are close to the Si-O-Si angles, 98.65° and 130.67°, in the stishovite crystal. Thus, the results for pair-distribution functions and bond-angle distributions at 4.28 g/cm^3 contain strong evidence for distorted $Si(O_{1/3})_6$ octahedra in the glass, joined at corners and sharing edges as well.

The ring statistics in SiO_2 glass has been calculated to gain insight into network topology. For a given Si atom, the shortest closed path of Si-O bonds defines a ring. In the normal density SiO_2 glass, there are no twofold rings (edge sharing tetrahedra) and the distribution is nearly symmetric with a peak at sixfold rings. As the density increases, there is a decrease in the number of sixfold rings and an increase in the population of smaller rings. At the stishovite density, there are only twofold, threefold, fourfold, and fivefold rings in the glass, similar to the ring distribution in stishovite crystal which has only twofold, threefold, and fourfold rings.

Based on the structural information, i.e., bond lengths, coordination numbers, bond-angle distributions, and static structure factor, as a function of density it is clear that our MD results at the density of 4.28 g/cm^3 are consistent with a "highly defective stishovite."

Finally, let us examine the effect of pressure on the phonon density of states (DOS) calculated with the knowledge of eigenvalues and eigenfunctions of the dynamical matrix. Figure 4 shows that the total DOS of SiO_2 glass at normal density has a broad band between 5 and 110 meV and a narrow band between 120 and 180 meV. The lower band has broad peaks at 20, 48, 66, and

93.9 meV while the higher band has narrow peaks at 139.5, 149.8, and 155.7 meV, in agreement with inelastic neutron scattering [6], infrared [14], and Raman [12,13] measurements. With an increase in the density, both bands shift to higher energies. When the glass density reaches the stishovite density, the two bands merge into a single broad band centered around 90 meV [Fig. 4(c)]. Similar changes have been observed in infrared and Raman spectra of SiO_2 glasses at high pressures [12–14].

At normal glass density, phonon modes between 5 and 100 meV are extended while the high-energy modes are localized. This is evident from the participation ratio [3], which is ~ 0.3 for phonons with energies between 5 and 80 meV and decreases sharply for high-energy modes. In the densified glass near the stishovite density, phonon modes remain extended up to 160 meV and localized near the band tails.

In conclusion, MD simulations provide a microscopic picture of changes in the short- and intermediate-range orders in the SiO_2 glass at high pressures. Under pressure, the FSDP decreases in height and moves to larger q values which cannot be accounted for by elastic compression. At a density of 2.64 g/cm^3, a new peak appears in $S(q)$ at $q = 2.85$ Å^{-1}. This peak grows as the density increases. At very high pressures, when the glass density reaches the stishovite density, the Si-O coordination increases to 5.8. The glass undergoes a transition from a corner sharing $Si(O_{1/2})_4$ tetrahedral network to a network of $Si(O_{1/3})_6$ octahedra jointed at corners and edges. This is in agreement with the recent high-pressure experiments on SiO_2 glass [16].

This work was supported by the U.S. Department of Energy, Office of Energy Research, Basic Energy Sciences, Materials Science Division, Grant No. DE-FG05-92ER45477. The computations were performed using the computing facilities in the Concurrent Computing Laboratory for Materials Simulations (CCLMS) at Louisiana State University.

[1] *The Physics and Technology of Amorphous SiO_2*, edited by R. A. B. Divine (Planeum, New York, 1988).

[2] S. C. Moss and D. L. Price, in *Physics of Disordered Materials*, edited by D. Adler, H. Fritzsche, and S. R. Ovshinksy (Plenum, New York, 1985), p. 77.

[3] R. J. Bell and D. C. Hibbins-Butler, J. Phys. C **8**, 878 (1975).

[4] P. A. V. Johnson, A. C. Wright, and R. N. Sinclair, J. Non-Cryst. Solids **58**, 109 (1983).

[5] P. N. Sen and M. F. Thorpe, Phys. Rev. B **15**, 4030 (1977).

[6] J. M. Carpenter and D. L. Price, Phys. Rev. Lett. **54**, 441 (1985).

[7] R. Dupree and R. F. Pettifer, Nature (London) **308**, 523 (1984).

[8] B. Feuston and S. H. Garofalini, J. Chem. Phys. **89**, 5818 (1988).

[9] P. Vashishta, R. K. Kalia, J. P. Rino, and I. Ebbsjö, Phys. Rev. B **41**, 12 197 (1990).

[10] S. R. Elliot, Nature (London) **354**, 445 (1991); Phys. Rev. Lett. **67**, 711 (1991).

[11] M. Grimsditch, Phys. Rev. Lett. **52**, 2379 (1984); Phys. Rev. B **34**, 4372 (1986); A. Polian and M. Grimsditch, Phys. Rev. B **41**, 6086 (1990).

[12] P. McMillan, B. Piriou, and R. Couty, J. Chem. Phys. **81**, 4234 (1984).

[13] R. J. Hemley, H. K. Mao, P. M. Bell, and B. O. Mysen, Phys. Rev. Lett. **57**, 747 (1986).

[14] Q. Williams and R. Jeanloz, Science **239**, 902 (1988).

[15] S. Susman *et al.*, Phys. Rev. B **43**, 1194 (1991).

[16] C. Meade, R. J. Hemley, and H. K. Mao, Phys. Rev. Lett. **69**, 1387 (1992).

[17] L. V. Woodcock, C. A. Angell, and P. Cheeseman, J. Chem. Phys. **65**, 1565 (1976).

[18] R. A. Murray and W. Y. Ching, Phys. Rev. B **39**, 1320 (1989).

[19] L. Stixrude and M. S. T. Bukowinski, Phys. Rev. B **44**, 2523 (1991).

[20] S. Tsuneyuki, Y. Matsui, H. Aoki, and M. Tsukada, Nature (London) **339**, 209 (1989).

[21] Y. Tsuchida and T. Yagi, Nature (London) **340**, 217 (1989).

[22] J. S. Tse and D. D. Klug, Phys. Rev. Lett. **67**, 3559 (1991); J. S. Tse, D. D. Klug, and Y. Le Page, Phys. Rev. Lett. **69**, 3647 (1992).

[23] N. Binggeli and J. R. Chelikowsky, Nature (London) **353**, 344 (1991); Phys. Rev. Lett. **69**, 2220 (1992).

[24] L. E. McNeil and M. Grimsditch, Phys. Rev. Lett. **68**, 83 (1992).

[25] Analytical forms of the two-body (V_2) and three-body (V_3) potentials are given by $V_2(i,j) = Q_iQ_j/r_{ij} - D_{ij}/r_{ij}^4 + H_{ij}/r_{ij}^{\eta_{ij}}$ and $V_3(i,j,k) = B_{jik}\exp[a/(r_{ij}-r_0)+a/(r_{ik}-r_0)](\cos\theta_{jik}-\cos\theta_{jik})^2\Theta(r_0-r_{ij})\Theta(r_0-r_{ik})$. See Ref. [9] for a complete discussion of V_2 and V_3 and the parameters in them.